

ARTICLES

Heat of Formation of the Hydroperoxyl Radical HOO Via Negative Ion Studies[†]

Tanya M. Ramond,^{‡,§} Stephen J. Blanksby,^{||} Shuji Kato,^{||} Veronica M. Bierbaum,^{*,||}
Gustavo E. Davico,[⊥] Rebecca L. Schwartz,[#] W. Carl Lineberger,^{*,‡,||} and G. Barney Ellison^{*,||}

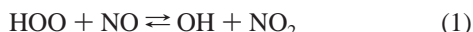
JILA, University of Colorado and National Institute of Standards and Technology,
Boulder, Colorado 80309-0440, and Department of Chemistry and Biochemistry,
University of Colorado, Boulder, Colorado 80309-0215

Received: December 19, 2001; In Final Form: May 13, 2002

We present a determination of $\Delta_f H_{298}(\text{HOO})$ based upon a negative ion thermodynamic cycle. The photoelectron spectra of HOO^- and DOO^- were used to measure the molecular electron affinities (*EAs*). In a separate experiment, a tandem flowing afterglow-selected ion flow tube (FA-SIFT) was used to measure the forward and reverse rate constants for $\text{HOO}^- + \text{HC}\equiv\text{CH} \rightleftharpoons \text{HOOH} + \text{HC}\equiv\text{C}^-$ at 298 K, which gave a value for $\Delta_{\text{acid}} H_{298}(\text{HOO}-\text{H})$. The experiments yield the following values: $EA(\text{HOO}) = 1.078 \pm 0.006$ eV; $T_0(\tilde{X} \text{HOO} - \tilde{A} \text{HOO}) = 0.872 \pm 0.007$ eV; $EA(\text{DOO}) = 1.077 \pm 0.005$ eV; $T_0(\tilde{X} \text{DOO} - \tilde{A} \text{DOO}) = 0.874 \pm 0.007$ eV; $\Delta_{\text{acid}} G_{298}(\text{HOO}-\text{H}) = 369.5 \pm 0.4$ kcal mol⁻¹; and $\Delta_{\text{acid}} H_{298}(\text{HOO}-\text{H}) = 376.5 \pm 0.4$ kcal mol⁻¹. The acidity/*EA* thermochemical cycle yields values for the bond enthalpies of $DH_{298}(\text{HOO}-\text{H}) = 87.8 \pm 0.5$ kcal mol⁻¹ and $D_0(\text{HOO}-\text{H}) = 86.6 \pm 0.5$ kcal mol⁻¹. We recommend the following values for the heats of formation of the hydroperoxyl radical: $\Delta_f H_{298}(\text{HOO}) = 3.2 \pm 0.5$ kcal mol⁻¹ and $\Delta_f H_0(\text{HOO}) = 3.9 \pm 0.5$ kcal mol⁻¹; we recommend that these values supersede those listed in the current NIST–JANAF thermochemical tables.

1. Introduction

The hydroperoxyl radical, HOO, is a key combustion intermediate in the oxidation of fuels¹ and plays a vital role in atmospheric chemistry as an oxidizer of volatile organic compounds.^{2,3} For these reasons, its thermochemistry is of great interest. There have been many independent determinations of the heat of formation of HOO, $\Delta_f H_{298}(\text{HOO})$, over the last few decades. For reviews, see those by Shum and Benson⁴ and more recently, by Fisher and Armentrout.⁵ Several early works reported low values of $\Delta_f H_{298}(\text{HOO})$, and this is reflected in the most recent NIST–JANAF table listing⁶ $\Delta_f H_{298}(\text{HOO}) = 0.50 \pm 2.01$ kcal mol⁻¹. There is strong evidence for a higher value of $\Delta_f H_{298}(\text{HOO})$ from radical kinetic studies.^{7,8} In 1980, k_1 and k_{-1} were measured by Howard⁷ as a function of temperature for the reaction



and the resulting K_{equi} (1) determined the free energy of reaction,

[†] Part of the special issue “Jack Beauchamp Festschrift”.

* To whom correspondence should be addressed. E-mail: veronica.bierbaum@colorado.edu, wcl@jila.colorado.edu, barney@jila.colorado.edu.

[‡] JILA.

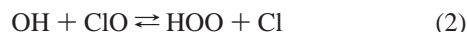
[§] Current address: NIST, MS 847-10, 325 Broadway, Boulder, Colorado 80305.

^{||} University of Colorado.

[⊥] Current address: Department of Chemistry, University of Idaho, Moscow, Idaho 83844-0001.

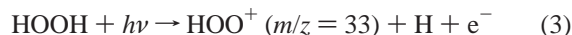
[#] Current address: Federal Bureau of Investigation Laboratory, Washington, D.C. 20535-0001.

$\Delta_{\text{rxn}} G_T$ (1), which in turn was used to derive $\Delta_f H_{298}(\text{HOO}) = 2.5 \pm 0.6$ kcal mol⁻¹. A second determination of $\Delta_f H_{298}(\text{HOO})$ by Hills and Howard⁸ involved a study of the reaction



that determined a somewhat higher value, $\Delta_f H_{298}(\text{HOO}) = 3.0 \pm 0.4$ kcal mol⁻¹. The value recommended by the “Chemical Kinetics and Photochemical Data for Use in Stratospheric Modeling” tables⁹, 2.8 ± 0.5 kcal mol⁻¹, was essentially an average of these two values. This value is widely accepted among those modeling atmospheric reactions, and another recent examination¹⁰ of reaction 2 finds the heat of formation of HOO in agreement with this averaged value.

Recently, a photoionization mass spectrometry (PIMS) experiment by Litorja and Ruscic¹¹ yielded values for the appearance energy of HOO^+ from HOOH , $AE(\text{HOO}^+, \text{HOOH})$, and the ionization energy of HOO, $IE(\text{HOO})$.



The values of $AE(\text{HOO}^+, \text{HOOH})$ and $IE(\text{HOO})$ imply that $\Delta_f H_{298}(\text{HOO}) = 3.3 \pm 0.8$ kcal mol⁻¹. In a similar vein, $\Delta_f H_{298}(\text{HOO}) = 3.8 \pm 1.2$ kcal mol⁻¹ is reported in a collision-induced dissociation threshold study by Fisher and Armentrout⁵. Although the $\Delta_f H_{298}(\text{HOO})$ measurements appear to be clustering around a value of about 3 kcal mol⁻¹, the precise value has not been established.

Ruscic et al. suggested recently that the heat of formation of the hydroxyl radical be revised from the longstanding values^{12,13} of $\Delta_f H_0(\text{OH}) = 9.35 \pm 0.05$ kcal mol⁻¹ and $\Delta_f H_{298}(\text{OH}) =$

$9.40 \pm 0.05 \text{ kcal mol}^{-1}$ to¹⁴ $\Delta_f H_0(\text{OH}) = 8.86 \pm 0.07 \text{ kcal mol}^{-1}$ and $\Delta_f H_{298}(\text{OH}) = 8.92 \pm 0.07 \text{ kcal mol}^{-1}$. From eqs 4 and 5, it is clear that a revision of $\Delta_f H_{298}(\text{OH})$ has implications for the heat of formation of the hydroperoxyl radical. An experimental derivation of $\Delta_f H_{298}(\text{HOO})$ depends on the measured $\Delta_{\text{rxn}} G_{298}$ of reactions 1 and 2 and also on the known heats of formation of the other reaction partners and products, which in both cases include the hydroxyl radical:

$$\Delta_f H_{298}(\text{HOO}) = \Delta_f H_{298}(\text{OH}) + \Delta_f H_{298}(\text{NO}_2) - \Delta_f H_{298}(\text{NO}) - \Delta_{\text{rxn}} H_{298} \quad (4)$$

$$\Delta_f H_{298}(\text{HOO}) = \Delta_f H_{298}(\text{OH}) + \Delta_f H_{298}(\text{ClO}) - \Delta_f H_{298}(\text{Cl}) + \Delta_{\text{rxn}} H_{298} \quad (5)$$

If $\Delta_f H_{298}(\text{OH})$ is revised, then the Howard values^{7–9} for $\Delta_f H_1(\text{HOO})$ must also be revised.

In this work, we present a measurement of $\Delta_f H_{298}(\text{HOO})$ that transcends the issues of the hydroxyl radical or the appearance energy curve onsets and instead depends only on negative ion thermochemistry.

We use the “acidity/*EA*” thermochemical cycle^{15,16} to measure the bond enthalpy of hydrogen peroxide, $DH_{298}(\text{HOO}-\text{H})$. If one measures the electron affinity of the hydroperoxyl radical, $EA(\text{HOO})$, and the enthalpy of deprotonation of $\text{HOO}-\text{H}$, $\Delta_{\text{acid}} H_{298}(\text{HOO}-\text{H})$, then one can complete the following cycle using the ionization energy of hydrogen, $IE(\text{H})$, to obtain the bond dissociation enthalpy of $\text{HOO}-\text{H}$, $DH_{298}(\text{HOO}-\text{H})$:

$$DH_{298}(\text{HOO}-\text{H}) = \Delta_{\text{acid}} H_{298}(\text{HOO}-\text{H}) - IE(\text{H}) + EA(\text{HOO}) + (\text{thermal correction}) \quad (6)$$

The thermal correction is needed because *EA* and *IE* are measured at 0 K. We measure the $\Delta_{\text{rxn}} G_{298}$ of the reaction between HOO^- and acetylene ($\text{HC}\equiv\text{C}-\text{H}$):



Through the relation

$$\Delta_{\text{rxn}} G_{298} = \Delta_{\text{acid}} G_{298}(\text{HC}\equiv\text{C}-\text{H}) - \Delta_{\text{acid}} G_{298}(\text{HOO}-\text{H}) \quad (8)$$

and a known value for the gas-phase acidity of acetylene, $\Delta_{\text{acid}} G_{298}(\text{HC}\equiv\text{C}-\text{H})$, $\Delta_{\text{acid}} G_{298}(\text{HOO}-\text{H})$ can be determined. Once the bond enthalpy $DH_{298}(\text{HOO}-\text{H})$ is extracted, the heat of formation of HOO , $\Delta_f H_{298}(\text{HOO})$, is calculated using well-known heats of formation of H and HOOH :

$$\Delta_f H_{298}(\text{HOO}) = DH_{298}(\text{HOO}-\text{H}) - \Delta_f H_{298}(\text{H}) + \Delta_f H_{298}(\text{HOO}-\text{H}) \quad (9)$$

In recent years, the bond enthalpy $DH_{298}(\text{HC}\equiv\text{C}-\text{H})$, from which the gas-phase acidity $\Delta_{\text{acid}} G_{298}(\text{HC}\equiv\text{C}-\text{H})$ can be extracted, has been measured precisely,¹⁷ and all other values involved in eqs 8 and 9 are known to great accuracy. Thus, it should be possible to improve both the accuracy and precision of the gas-phase acidity value of HOOH that was previously reported by our laboratory.¹⁸

Although HOO has been studied thoroughly via negative ion photoelectron spectroscopy,^{19,20} the only photoelectron spectrum of DOO^- was measured with an early photoelectron spectrometer about 15 years ago.¹⁹ Our current spectrum slightly revises the most recent determination of $EA(\text{HOO})$,²⁰ which is then used to calculate thermochemical quantities as outlined in eq 6 above.

In addition, we present the photoelectron spectrum of DOO^- and its electron affinity (*EA*), term energy $T_0(\tilde{A} \leftarrow \tilde{X})$, as well as vibrational frequencies in both the \tilde{X} and \tilde{A} states of DOO .

2. Experimental Section

A. Negative Ion Photoelectron Spectroscopy. The photoelectron spectrometer used in this experiment has been described elsewhere,^{21,22} but a brief overview is given here. DOO^- anions were created in a microwave discharge source by introducing the vapor above a mixture of HOOH and D_2SO_4 in D_2O . Enough HOOH remained in the solution to enable the generation of HOO^- anions using the same sample. The anions were thermalized in a flow tube that could be cooled with liquid nitrogen to give 200 K sample ions. The ions were gently extracted into a differentially pumped region, accelerated through a Wien velocity filter, and then decelerated into an interaction region where they intersected the beam of a fixed-frequency 364-nm CW laser. The kinetic energy of the photoelectrons was recorded using a hemispherical energy analyzer and a position-sensitive detector. Typical resolution was around 8 meV. A half-wave plate in the beam path of the laser was used to vary the polarization angle and allows photoelectron angular distribution measurements.²³

B. Flowing Afterglow-Selected Ion Flow Tube Measurements. The gas-phase acidity of HOOH was measured using a tandem flowing afterglow-selected ion flow tube (FA-SIFT) apparatus that had been previously described.²⁴ The acidity was established by measurement of the rate constant for proton transfer between HOO^- and acetylene, which is shown in reaction 7, coupled with the measurement of the rate constant for the reverse reaction. Measurements were conducted at 298 K. The ratio of the two measured rate constants, k_f and k_r , gives the proton-transfer equilibrium constant, K_{equi} , which is related to the difference in the gas-phase acidities of $\text{HOO}-\text{H}$ and $\text{HC}\equiv\text{C}-\text{H}$ by the simple expression in eq 10. Given the gas-phase acidity of acetylene at 298 K, $\Delta_{\text{acid}} G_{298}(\text{HC}\equiv\text{C}-\text{H})$, the gas-phase acidity of $\text{HOO}-\text{H}$ can be extracted from eq 10.

$$\Delta_{\text{acid}} G_{298}(\text{HOO}-\text{H}) - \Delta_{\text{acid}} G_{298}(\text{HC}\equiv\text{C}-\text{H}) = \Delta \Delta_{\text{acid}} G_{298} = RT \ln K_{\text{equi}} \quad (10)$$

All rate constants reported in this article are presented with their associated statistical uncertainties along with other errors (e.g., those arising from mass discrimination and sample decomposition). It should be noted that these uncertainties do not include systematic errors due to temperature, flow rates, and pressure measurements. Systematic errors of this kind will be the same for the measurement of forward and reverse rate constants and therefore need not be considered in the determination of K_{equi} and its associated uncertainty. However, the overall uncertainty for any given rate constant will typically be $\pm 20\%$, where statistical and other errors are smaller than 20%.

For the forward reaction, HOO^- anions were prepared by collision-induced dissociation of $t\text{-BuOO}^-$ anions. The $t\text{-BuOO}^-$ anions were generated in the first flow tube by reaction of $t\text{-BuOOH}$ with hydroxide ions and were then injected into the second flow tube at relatively high injection potentials ($E_{\text{LAB}} > 30 \text{ eV}$). At these energies, collisions between the $t\text{-BuOO}^-$ ions and the helium buffer gas in the second flow tube (0.5 Torr) cause complete dissociation of the precursor ion to produce HOO^- anions exclusively.^{25,26} The acetylene ($\text{HC}\equiv\text{CH}$, Matheson) used for this reaction was passed through a stainless steel coil cooled to $-78 \text{ }^\circ\text{C}$ in a dry ice–acetone bath to remove trace acetone from the sample.²⁷ For the reverse reaction,

$\text{HC}\equiv\text{C}^-$ anions were produced by the reaction of acetylene with hydroxide ions in the first flow tube. The mass-selected ions then react with HOOH vapor in the second flow tube. The HOOH sample was prepared by concentrating commercial 70% HOOH by bubbling dry nitrogen through the sample over a period of several weeks. The peroxide concentration in the liquid phase was determined to be $94 \pm 1\%$ by titration against a standard aqueous solution of acidified KMnO_4 . The vapor composition above a $94 \pm 1\%$ hydrogen peroxide solution has been measured to be $75 \pm 5\%$ hydrogen peroxide at 298 K.²⁸ The actual concentration of HOOH in the vapor present in the second flow tube was determined experimentally by two methods discussed in detail below. Using both techniques, we found the concentration of HOOH vapor to be considerably lower than 75%, even after a steady-state concentration of HOOH in the second flow tube had been attained, suggesting decomposition of HOOH both in the inlet system and in the flow tube with concomitant formation of nonreactive water and dioxygen molecules. Consequently, measurements of k_r (reaction 7) were bracketed by the HOOH calibration experiments.

Two different experiments were conducted to quantify the amount of hydrogen peroxide available for reaction with ions in the second flow tube. (A) First, the rate of reaction of hydroxide ions with the hydrogen peroxide vapor was measured using flow rates of HOOH vapor that were identical to those used for the acetylide experiments.



The apparent rate coefficient for the proton transfer depicted in reaction 11, under the same influence of nonreactive impurities, was measured to be $k_{\text{apparent}} = (3.33 \pm 0.46) \times 10^{-10} \text{ cm}^3 \text{ molecule}^{-1} \text{ s}^{-1}$. This value includes the small correction (8%) for secondary regeneration of hydroxide ions ($\text{HOO}^- + \text{HOOH} \rightarrow \text{H}_2\text{O} + \text{O}_2 + \text{HO}^-$). The measured rate coefficient represents only 14% of the calculated collision rate, $k_{\text{collision}} = 2.47 \times 10^{-9} \text{ cm}^3 \text{ molecule}^{-1} \text{ s}^{-1}$. Reaction 11 involves highly localized anions and is exothermic^{34,41} by at least 14 kcal mol⁻¹; therefore, the reaction is expected to proceed at the collision rate.⁴² Taking the ratio of the calculated collision and the measured rates for reaction 11, we can scale the measured rate constant for the acetylide reaction ($\text{HC}\equiv\text{C}^- + \text{HOOH} \rightarrow \text{HC}\equiv\text{CH} + \text{HOO}^-$). This scaling gives the upper limit for the rate constant k_r in reaction 7.

(B) In a second experiment, SIFT-injected DO^- ions were reacted with the HOOH vapor mixture from a given inlet at the same flow rate as that used in the previous two experiments. The reaction produced HO^- (51%) and HOO^- (49%) along with a very minor amount of DOO^- (<0.5%). The depletion of the DO^- signal ($[\text{DO}^-]/[\text{DO}^-]_0$) can be rationalized in terms of two competing reactions: (i) deprotonation of HOOH (reaction 11) and (ii) a rapid H/D exchange reaction to produce HO^- ions as indicated in reaction 12. Other DO^- loss processes due to H/D scrambling in the $\text{DO}^- + \text{HOOH}$ collision should be negligible, as indicated by the minimal amount of DOO^- detected.



The depletion due only to deprotonation of HOOH can be accounted for by examining the depletion for the analogous HO^- reaction ($[\text{HO}^-]/[\text{HO}^-]_0$). Thus, the ratio of $[\text{DO}^-]/[\text{DO}^-]_0$ to $[\text{HO}^-]/[\text{HO}^-]_0$, measured under identical conditions, gives the depletion of DO^- that is dependent only on reaction 12. To calibrate the amount of water in the HOOH vapor mixture, DO^- was then reacted with pure water from the same inlet with

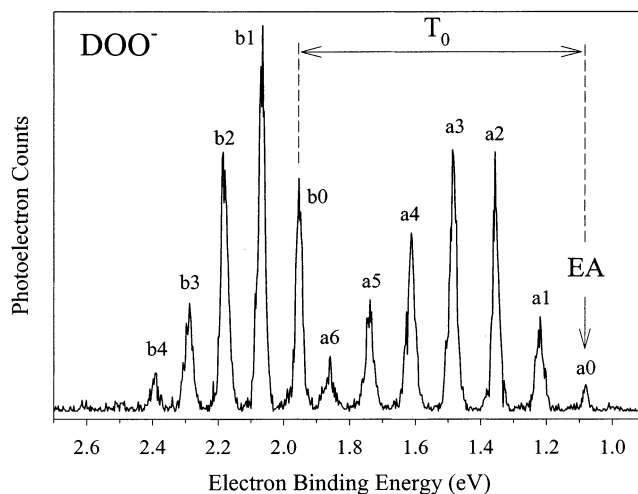


Figure 1. Photoelectron spectrum (at 364 nm) of DOO^- taken at a 200 K source temperature with magic angle laser polarization.

various flow rates until a match for the previously determined depletion was obtained. From this calibration, we conclude that this mixture contains 70% water vapor. We can scale the measured rate constant for the acetylide reaction taking the amount of this water impurity into account. Because this calibration method (B) measures only water and not dioxygen, this scaling gives a conservative lower bound for k_r in reaction 7.

3. Results

A. Negative Ion Photoelectron Spectroscopy of HOO^- and DOO^- . The magic angle 364-nm photoelectron spectrum of DOO^- taken at a 200 K sample temperature is shown in Figure 1. Comparison between 300 K (not shown) and 200 K spectra confirms that there are no hot bands in this spectrum. The spectrum clearly shows two different Franck–Condon envelopes, suggesting transitions into two different electronic states of the neutral molecule. Peaks **a0**–**a6** have an interpeak spacing of about 1100 cm^{-1} , peaks **b0**–**b4** have an approximate 900- cm^{-1} separation, and the spacing between peaks **a6** and **b0** is about 740 cm^{-1} . Because of this spacing, peak **b0** is determined to be the vibrational origin (0_0^0) of the $\tilde{X} \text{HOO}^-$ to $\tilde{A} \text{HOO}^-$ transition. It is not immediately obvious which peak should be assigned as the electron affinity peak; because the Franck–Condon profile maximizes around peak **a3**, the EA transition, falling to the lower binding-energy side of peak **a0**, might have been too weak for us to detect. However, the term energy of the \tilde{A} state is known to great precision (7018 cm^{-1}),²⁹ and this value is also the interval between peaks **a0** and **b0** (7025 \pm 40 cm^{-1}). Therefore, the electron affinity transition may be assigned with confidence as corresponding to peak **a0**, yielding $EA(\text{DOO}) = 1.077 \pm 0.005 \text{ eV}$ and a term energy of $T_0(\tilde{X} \text{DOO} - \tilde{A} \text{DOO}) = 0.874 \pm 0.005 \text{ eV}$ (see Table 1). This EA value agrees with the photoelectron spectroscopy value given in Oakes et al. of 1.089 \pm 0.017 eV,¹⁹ although with significantly reduced error bars.

The photoelectron spectrum of HOO^- has been reported recently by Clifford et al. with an EA of 1.089 \pm 0.006 eV.²⁰ However, a sign error was made in the rotational correction to the raw EA value. The correct value²² is $EA(\text{HOO}) = 1.078 \pm 0.006 \text{ eV}$ with $T_0(\tilde{X} \text{HOO} - \tilde{A} \text{HOO}) = 0.872 \pm 0.005 \text{ eV}$; this is the most current and most accurate measurement available (see Table 1). These values are the same, within error, as those reported for DOO above, as would be expected.

TABLE 1: Data Extracted from the 364-nm Photoelectron Spectra of HOO⁻ and DOO⁻^{a,b}

	EA (eV)	T ₀ (eV)	β	ω _{O-O} (cm ⁻¹)	x _{O-O} (cm ⁻¹)	ν _{O-O} (cm ⁻¹)
HOO \tilde{X}^2A''	1.078(6)	0	-0.7(1)	1125(6)	11(1)	1102(10)
HOO \tilde{A}^2A'		0.872(5)	-0.5(1)	921(4)	5(1)	910(7)
DOO \tilde{X}^2A''	1.077(5)	0	-0.7(1)	1138(4)	13(1)	1112(7)
DOO \tilde{A}^2A'		0.874(5)	-0.5(1)	955(6)	13(2)	929(10)

^a EA, electron affinity; T₀, term energy; β, anisotropy parameter; ω_{O-O}, O–O harmonic vibrational frequency; x_{O-O}, O–O anharmonicity; ν_{O-O}, O–O fundamental vibrational frequency. See eq 13. ^b The methods used to extract these values and their associated uncertainties (given in parentheses) are discussed in the text.

Peaks **a1–a6** represent transitions into six quanta of a single vibrational mode in the \tilde{X} state of DOO. Likewise, peaks **b1–b4** represent a single progression of four quanta of vibrational excitation in the \tilde{A} state. Because of the number of well-resolved peaks in this spectrum, the measured energy spacings ($G(v) - G(0)$ where $v = 1-6$ (or 4) of modes **a** (or **b**)) between all these peaks with respect to the appropriate 0₀⁰ peak (**a2–a0**, **a3–a0**, **a4–a0**, etc.) were fitted³⁰ to eq 13 using a weighted least-squares approach:

$$G(v) - G(0) = \omega\left(v + \frac{1}{2}\right) - x\left(v + \frac{1}{2}\right)^2 - \frac{\omega}{2} + \frac{x}{4} \quad (13)$$

Fitting the **a** progression data to eq 13 gives the harmonic frequency of mode **a**, ω_a = 1138 ± 4 cm⁻¹, and an anharmonicity, x_a = 13 ± 1 cm⁻¹. Using these parameters, we can extract an accurate value for the 1 ← 0 vibrational transition of mode **a**, ν_a = 1112 ± 7 cm⁻¹. Doing the same for mode **b** yields ω_b = 955 ± 6 cm⁻¹, x_b = 13 ± 2 cm⁻¹, and ν_b = 929 ± 10 cm⁻¹.

The same photoelectron spectrum analysis discussed above is applied to HOO⁻, with the results reported in Table 1 (for further details, see ref 22). What is important to note is that the normal mode fundamentals in both electronic states do not change significantly upon deuteration. If a normal mode includes the motion of a hydrogen atom, its frequency would decrease upon substitution of H for D. Thus, deuteration of the HOO molecule and comparing the spectra of the two isotopomers allows confirmation that the vibrational activity in the photoelectron spectra of HOO⁻ and DOO⁻ does not involve hydrogen motion. The only possible vibrational mode candidate then is ν₃, the O–O stretch. There is little evidence from the photoelectron spectra of any significant mixing of the O–O stretch and the HOO bend, as has been previously suggested.³¹

The 929 ± 10 cm⁻¹ value of ν₃ in the \tilde{A} state of DOO matches the 930 cm⁻¹ frequency reported in the photoelectron spectroscopy study of Oakes et al.¹⁹ However, the Oakes et al. ground-state measurement¹⁹ of DOO ν₃ (1020 cm⁻¹) does not agree with the value of the ground-state ν₃ mode of DOO presented here, ν₃(DOO \tilde{X}) = 1112 ± 7 cm⁻¹. Our \tilde{X} ν₃ value does agree with those of McKellar³² (1120.22 cm⁻¹) and Smith and Andrews³³ (1123.2 cm⁻¹), and it is likely to be a more reliable measurement than the earlier measurement of Oakes et al.¹⁹ because of a cooler ion source and improved resolution.

The extended progression in the O–O stretch seen in both the HOO⁻ and DOO⁻ photoelectron spectra testifies to a relatively large change in the O–O bond length upon electron detachment from the anion, as has been discussed in Clifford et al.²⁰ and Ramond²² as well as in Blanksby et al.³⁴ with respect to the CH₃OO⁻ and CH₃CH₂OO⁻ alkyl peroxides. Absence of the bending vibration indicates that the photoelectron detachment is a process that is fairly localized to an orbital on the terminal

oxygen. In the case of OO⁻, the orbital would be a pure π orbital. Detachment of an electron from this orbital with 350-nm radiation results in a photoelectron angular distribution that is peaked perpendicular to the laser polarization vector (i.e., the anisotropy parameter β is between 0 and -1).³⁵ The measured anisotropy values for both HOO⁻ and DOO⁻ (Table 1) are strongly peaked perpendicular to the laser polarization, supporting the identification of the orbital from which detachment occurs and indicating that the simple π nature of this orbital is not severely perturbed by the presence of the hydrogen atom.

B. Gas-Phase Acidity. The reaction of HOO⁻ with acetylene formed predominantly (92%) the expected proton-transfer product (reaction 14) along with small amounts of the [HOO⁻⋯HC≡CH] cluster ion (~4%) and an anion at *m/z* 41, presumably HC≡CO⁻ (~4%).



The overall rate of the forward reaction of HOO⁻ with acetylene (reaction 14) was measured to be slow, with a rate constant of $k_{\text{overall}} = (2.54 \pm 0.08) \times 10^{-10} \text{ cm}^3 \text{ molecule}^{-1} \text{ s}^{-1}$, which is less than 25% of the calculated collision rate³⁷ of $k_{\text{collision}} = 1.12 \times 10^{-9} \text{ cm}^3 \text{ molecule}^{-1} \text{ s}^{-1}$. This value suggests a slightly endothermic proton transfer that is consistent with the observed formation of [HOO⁻⋯HC≡CH] in addition to HC≡C⁻. The product ions [HOO⁻⋯HC≡CH] and HC≡CO⁻ account for ~8% of the total ion count. If we assume that these species are formed from the endothermic fraction of the thermal ion population (i.e., those ions with insufficient energy to undergo proton transfer), then we can correct the proton-transfer rate to give a best value for $k_{14} = (2.34 \pm 0.07) \times 10^{-10} \text{ cm}^3 \text{ molecule}^{-1} \text{ s}^{-1}$ (21% of the collision rate).

The reverse reaction of HC≡C⁻ with hydrogen peroxide (reaction 15) gave predominantly HOO⁻ ions by proton transfer; no clustering between HOOH and HC≡C⁻ was observed.



Hydroxide ions were also formed, but in relatively low abundance; the OH⁻ signal was approximately 8% of the HOO⁻ signal under the experimental conditions, which used a fairly low concentration of HOOH. These ions were attributed to the secondary reaction (eq 16) that has been previously reported.¹⁸



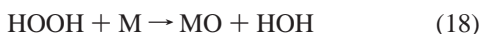
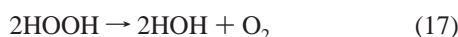
The apparent reaction rate constant for reaction 15 was measured to be $k_{\text{apparent}} = (1.98 \pm 0.30) \times 10^{-10} \text{ cm}^3 \text{ molecule}^{-1} \text{ s}^{-1}$. This value is only 9% of the calculated collision rate³⁷ of $k_{\text{collision}} = 2.19 \times 10^{-9} \text{ cm}^3 \text{ molecule}^{-1} \text{ s}^{-1}$. This value is considerably smaller than expected from the exothermicity of the proton transfer, which is anticipated from (i) the slowness of the forward reaction (eq 14) and (ii) the observation of clustering in the forward but not in the reverse (eq 15) reactions. As previously stated, the gas-phase concentration of HOOH is substantially lower than the predicted value of 75%, giving rise to apparently slow reaction 15.

Literature reports estimate that the vapor above a 94 ± 1% aqueous hydrogen peroxide solution is 75 ± 5% HOOH at room temperature.²⁸ The remaining 25 ± 5% is water, which is unreactive toward the acetylide anion. Thus, we can correct the measured rate to be $k_{\text{corrected}} = 2.65 \times 10^{-10} \text{ cm}^3 \text{ molecule}^{-1} \text{ s}^{-1}$. However, this value represents only 12% of the calculated collision rate. This low reaction rate is explained by the decomposition of the hydrogen peroxide, which decreases the

TABLE 2: Entropies and Enthalpies Taken from Gurvich et al.¹²

species	$H^\circ(298) - H^\circ(0)$ (kcal mol ⁻¹)	$S^\circ(298)$ (cal mol ⁻¹ K ⁻¹)	$\Delta_f H_{298}$ (kcal mol ⁻¹)
HOOH	2.667	56.051	-32.48 ± 0.05
HOO	2.391		
HOO ⁻	2.394	53.562	
O ₂	2.075		
H ₂	2.024		
H	1.481		52.1028 ± 0.0014
H ⁺	1.481	26.039	

actual HOOH concentration in the gas phase. Two decomposition mechanisms are possible: (i) surface-catalyzed decomposition³⁸ to oxygen and water (eq 17) and (ii) metal (M) oxidation³⁹ to form metal oxide and water (eq 18). Such chemistry would likely be facilitated by contact between the HOOH vapor and the metal and glass surfaces of the inlet system and the second flow tube.⁴⁰



The calibration experiment (A) gives an upper bound (see Experimental Section) for the rate coefficient of reaction 15 of $k_{15A} = (1.47 \pm 0.05) \times 10^{-9}$ cm³ molecule⁻¹ s⁻¹, which is 67% of the calculated collision rate and is more indicative of an exothermic proton-transfer reaction. A conservative lower bound for the rate coefficient of reaction 15 obtained from experiment (B) is $k_{15B} = (6.6 \pm 1.0) \times 10^{-10}$ cm³ molecule⁻¹ s⁻¹. This latter value is 30% of the calculated collision rate.

These two experiments give a range of values for the corrected rate constants k_{15A} and k_{15B} . By combining each of these values with the reliably measured k_{14} and using eq 10, we can derive the following values for the gas-phase acidity of hydrogen peroxide: $\Delta_{\text{acid}}G_{298}(\text{HOO}-\text{H})_A = 369.2$ kcal mol⁻¹ and $\Delta_{\text{acid}}G_{298}(\text{HOO}-\text{H})_B = 369.7$ kcal mol⁻¹. We note that most systematic errors in rate constant determinations cancel in these calculations. Therefore, the values of $\Delta_{\text{acid}}G_{298}(\text{HOO}-\text{H})_A$ and $\Delta_{\text{acid}}G_{298}(\text{HOO}-\text{H})_B$ represent lower and upper bounds, respectively, for the true value of the gas-phase acidity. We recommend a best value of $\Delta_{\text{acid}}G_{298}(\text{HOO}-\text{H}) = 369.5 \pm 0.4$ kcal mol⁻¹, where the associated uncertainty arises primarily from the uncertainty associated with the reference acetylene⁴³ (370.3 ± 0.3 kcal mol⁻¹).

C. Entropy and Enthalpy Determinations. The $\Delta_{\text{acid}}H_{298}(\text{HOO}-\text{H})$ term in eq 6 can be extracted from the experimentally determined $\Delta_{\text{acid}}G_{298}(\text{HOO}-\text{H})$ value and the entropy of deprotonation $\Delta_{\text{acid}}S_{298}(\text{HOO}-\text{H})$ via the simple relation in eq 19.

$$\Delta_{\text{acid}}H_{298}(\text{HOO}-\text{H}) = \Delta_{\text{acid}}G_{298}(\text{HOO}-\text{H}) + T\Delta_{\text{acid}}S_{298}(\text{HOO}-\text{H}) \quad (19)$$

The entropy of deprotonation can be determined using entropies (S_{298}) given in the compilation of Gurvich et al.¹² and listed in Table 2 (unless otherwise stated, all supplementary thermochemical values are those given by Gurvich et al.¹² and are listed for convenience in Table 2). This gives $\Delta_{\text{acid}}S_{298}(\text{HOO}-\text{H}) = 23.5 \pm 0.5$ cal mol⁻¹ K⁻¹ and thus $\Delta_{\text{acid}}H_{298}(\text{HOO}-\text{H}) = 376.5 \pm 0.4$ kcal mol⁻¹.

The thermal correction in eq 6 corresponds to the sum of the integrated heat capacities, which is always small (≤ 0.3 kcal mol⁻¹) and is therefore often ignored.¹⁵ However, in this article, we evaluate this term explicitly using the integrated heat

capacities listed in Table 2.

$$\text{thermal correction} = \int_0^{298} dT (C_p[\text{HOO}] - C_p[\text{HOO}^-] + C_p[\text{H}] - C_p[\text{H}^+]) \quad (20)$$

Including this correction, we derive a bond enthalpy for hydrogen peroxide of $DH_{298}(\text{HOO}-\text{H}) = 87.8 \pm 0.5$ kcal mol⁻¹. The bond dissociation energy can be derived from the bond enthalpy at 298 K using eq 21. The integrated heat capacities are listed in Table 2.¹² This calculation yields a bond energy for hydrogen peroxide of $D_0(\text{HOO}-\text{H}) = 86.6 \pm 0.5$ kcal mol⁻¹.

$$D_0(\text{HOO}-\text{H}) = DH_{298}(\text{HOO}-\text{H}) - \int_0^{298} dT (C_p[\text{HOO}] + C_p[\text{H}] - C_p[\text{HOOH}]) \quad (21)$$

Equation 22 uses (i) the bond enthalpy derived above and (ii) the heats of formation of hydrogen peroxide and the hydrogen radical (Table 2) to give the heat of formation of the hydroperoxyl radical at 298 K, $\Delta_f H_{298}(\text{HOO}) = 3.2 \pm 0.5$ kcal mol⁻¹. This value may be corrected for the integrated heat capacity as shown in eq 23 to give the heat of formation of the hydroperoxyl radical at 0 K, $\Delta_f H_0(\text{HOO}) = 3.9 \pm 0.5$ kcal mol⁻¹.

$$\Delta_f H_{298}(\text{HOO}) = DH_{298}(\text{HOO}-\text{H}) + \Delta_f H_{298}(\text{HOOH}) - \Delta_f H_{298}(\text{H}) \quad (22)$$

$$\Delta_f H_0(\text{HOO}) = \Delta_f H_{298}(\text{HOO}) - \int_0^{298} dT (C_p[\text{HOO}] - 0.5C_p[\text{H}_2] - C_p[\text{O}_2]) \quad (23)$$

Finally, eq 24 can be used with (i) the bond energy of hydrogen peroxide derived above and (ii) the ionization energy of the hydroperoxyl radical, $IE(\text{HOO}) = 11.352 \pm 0.007$ eV, from Litorja and Ruscic¹¹ to calculate the appearance energy of the HOO⁺ cation from HOOH, $AE(\text{HOO}^+, \text{HOOH}) = 348.4 \pm 0.5$ kcal mol⁻¹ (15.11 ± 0.02 eV):

$$AE(\text{HOO}^+, \text{HOOH}) = D_0(\text{HOO}-\text{H}) + IE(\text{HOO}) \quad (24)$$

A summary of all derived thermochemical values presented here is given in Table 4.

4. Discussion

A. Comparison with Previous Thermochemical Determinations. Previously, we¹⁸ measured the enthalpy of deprotonation for hydrogen peroxide in a flowing afterglow apparatus using the equilibria outlined in reactions 25 and 26. These experiments proved extremely challenging because some of these reactions



are extremely slow and thus difficult to measure. However, the final reported value of $\Delta_{\text{acid}}H_{298}(\text{HOOH}) = 375.5 \pm 3.3$ kcal mol⁻¹ is in good agreement with the more precise FA-SIFT result detailed above.

Our result for the heat of formation of the hydroperoxyl radical is in reasonable agreement with the value recommended in the review article of Shum and Benson,⁴ $\Delta_f H_{298}(\text{HOO}) =$

TABLE 3: Comparison of the Heats of Formation for the Hydroperoxyl Radical, $\Delta_f H_0(\text{HOO})$ and $\Delta_f H_{298}(\text{HOO})$

data source	reference	$\Delta_f H_0(\text{HOO})$ (kcal mol ⁻¹)	$\Delta_f H_{298}(\text{HOO})$ (kcal mol ⁻¹)
NIST-JANAF tables	6	1.2 ± 2.0	0.5 ± 2.0
Gurvich et al.'s tables	12	3.0 ± 0.7	2.3 ± 0.7
HOO + NO ⇌ HO + NO ₂	recalculation ^a using ref 7 and $\Delta_f H_T(\text{OH})$ from ref 12	3.2 ± 0.4	2.5 ± 0.4
HOO + NO ⇌ HO + NO ₂	recalculation ^a using ref 7 and $\Delta_f H_T(\text{OH})$ from ref 14	2.7 ± 0.4	2.0 ± 0.4
HO + ClO ⇌ HOO + Cl	recalculation ^a using ref 8 and $\Delta_f H_T(\text{OH})$ from ref 12	4.1 ± 0.2	3.4 ± 0.2
HO + ClO ⇌ HOO + Cl	recalculation ^a using ref 8 and $\Delta_f H_T(\text{OH})$ from ref 14	3.6 ± 0.2	2.9 ± 0.2
O ₂ ⁺ + CH ₄ → CH ₃ ⁺ + HO ₂ collision-induced threshold study	5		3.8 ± 1.2
PIMS/AE ^b positive ion cycle	11	4.0 ± 0.8	3.3 ± 0.8
acidity/EA cycle	this work	3.9 ± 0.5	3.2 ± 0.5

^a See text and Supporting Information for details. ^b Photoionization mass spectrometry/appearance energy.

TABLE 4: Recommended Thermochemical Quantities^a

quantity	0 K	298 K
EA(HOO)	24.9 ± 0.1	
$\Delta_{\text{acid}} G_T(\text{HOOH})$		369.5 ± 0.4
$\Delta_{\text{acid}} H_T(\text{HOOH})$		376.5 ± 0.4
$DH_T(\text{HOO}-\text{H})$	86.6 ± 0.5	87.8 ± 0.5
$\Delta_f H_T(\text{HOO})$	3.9 ± 0.5	3.2 ± 0.5

^a All values are in kcal mol⁻¹

3.5^{+1.0}_{-0.5} kcal mol⁻¹, and with the value derived by Fisher and Armentrout,⁵ $\Delta_f H_{298}(\text{HOO}) = 3.8 \pm 1.2$ kcal mol⁻¹. Our new heat of formation falls within the stated uncertainty of the $\Delta_f H_{298}(\text{HOO}) = 2.8 \pm 0.5$ kcal mol⁻¹ value recommended by Howard and co-workers⁹ and also overlaps with the number chosen for the most recent Gurvich thermochemical tables,¹² which was based on the Howard experiments⁷ (Table 3). The Litorja and Ruscic measurement¹¹ of the bond dissociation energy, $D_0(\text{HOO}-\text{H}) = 86.7 \pm 0.8$ kcal mol⁻¹, is in excellent agreement with our value. Their extracted heats of formation of the hydroperoxyl radical, $\Delta_f H_0(\text{HOO}) = 4.0 \pm 0.8$ kcal mol⁻¹ and $\Delta_f H_{298}(\text{HOO}) = 3.3 \pm 0.8$ kcal mol⁻¹, are also in excellent agreement with those that we derive in this work. The high level of agreement between our results and the result from these completely different experimental approaches is a gratifying outcome and suggests that the heat of formation of the peroxy radical has now been established with some confidence. Furthermore, our experiments have substantially reduced the uncertainty associated with this value.

B. Implications for the Heats of Formation of the Hydroxyl Radical. We use the data reported by both Howard⁷ and Hills and Howard⁸ and auxiliary thermochemical values from the tables of Gurvich et al.,¹² which are the most accurate and current thermochemical tables, to compute $\Delta_f H_0(\text{HOO})$ and $\Delta_f H_{298}(\text{HOO})$. Then we repeat the calculation but instead use the most current values of $\Delta_f H_0(\text{OH})$ and $\Delta_f H_{298}(\text{OH})$ to date¹⁴ (Table 3). As can be seen from Table 3, the values with the most recent $\Delta_f H_T(\text{OH})$ ¹⁴ are consistently lower than those without the most recent $\Delta_f H_T(\text{OH})$ ¹⁴ by 0.5 kcal mol⁻¹, as would be expected. The details of how these data were computed, along with additional relevant calculations, are presented in Supporting Information.

Comparison of the various $\Delta_f H_T(\text{HOO})$ values (Table 3) shows better agreement between our extracted values and the values calculated with the $\Delta_f H_T(\text{OH})$ originally reported¹² than

with those calculated with the most recent values of $\Delta_f H_T(\text{OH})$.¹⁴ This casts some doubt on the revised value of $\Delta_f H_T(\text{OH})$. However, it should be pointed out that the uncertainties of our measurements and those of Howard and co-workers^{8,7} are still too large to permit definitive assignment of the heat of formation of the hydroxyl radical.

5. Conclusions

We have measured the enthalpy of deprotonation of HOOH and have recorded the photoelectron spectra of HOO⁻ and DOO⁻. Using a negative ion thermodynamic cycle, which is a method independent of the recently questioned thermodynamics of OH or the difficulties involved in threshold experiments, we have calculated the heat of formation of HOO. Our derived number agrees nicely with existing literature values obtained through various alternative methods and has smaller uncertainty, which implies that we have a definitive value for the heat of formation of HOO.

Acknowledgment. S.J.B. and G.B.E. are pleased to acknowledge support by the Chemical Physics Program, United States Department of Energy (DE-FG02-87ER13695); G.B.E. is a Fellow of the J.S. Guggenheim Foundation. W.C.L. is pleased to acknowledge support from the National Science Foundation and the Air Force Office of Scientific Research. V.M.B. and S.K. gratefully acknowledge support from the National Science Foundation (CHE 0100664). We thank David McCabe for assistance with the purification and titration of hydrogen peroxide. We also thank Dr. Carleton J. Howard at NOAA, Dr. Branko Ruscic at Argonne National Laboratory, and Dr. Geoff Tyndall at NCAR for useful discussions.

Supporting Information Available: The results and details of the recalculation of $\Delta_f H_T(\text{HOO})$, $DH_T(\text{HOO}-\text{H})$, and $\Delta_{\text{acid}} H_T(\text{HOO}-\text{H})$ starting with data from Howard⁷ as well as that from Hills and Howard⁸ using $\Delta_f H_T(\text{OH})$ from both thermochemical tables as well as the recent work of Ruscic et al.¹⁴ This material is available free of charge via the Internet at <http://pubs.acs.org>.

References and Notes

- (1) Warnatz, J. Rate Coefficients in the C/H/O System. In *Combustion Chemistry*; Gardiner, W. C., Jr., Ed.; Springer-Verlag: New York, 1984.

- (2) Seinfeld, J. H.; Pandis, S. N. *Atmospheric Chemistry and Physics: From Air Pollution to Climate Change*; Wiley & Sons: New York, 1998.
- (3) Bohn, B.; Zetzsch, C. *J. Phys. Chem. A* **1997**, *101*, 1488.
- (4) Shum, L. G. S.; Benson, S. W. *J. Phys. Chem. A* **1983**, *87*, 3479.
- (5) Fisher, E. R.; Armentrout, P. B. *J. Phys. Chem. A* **1990**, *94*, 4396.
- (6) Chase, M. W., Jr.; Davies, C. A.; Downey, J. R., Jr.; Frurip, D. J.; McDonald, R. A.; Syverud, A. N. *NIST-JANAF Thermochemical Tables*, 4th ed.; American Chemical Society: Washington, DC, 1998.
- (7) Howard, C. J. *J. Am. Chem. Soc.* **1980**, *102*, 6937.
- (8) Hills, A. J.; Howard, C. J. *J. Chem. Phys.* **1984**, *81*, 4458.
- (9) DeMore, W. B.; Sander, S. P.; Golden, D. M.; Hampson, R. F.; Kurylo, M. J.; Howard, C. J.; Ravishankara, A. R.; Kolb, C. E.; Molina, M. J. *Chemical Kinetics and Photochemical Data for Use in Stratospheric Modeling: Evaluation Number 12*; National Aeronautics and Space Administration, Jet Propulsion Laboratory: Pasadena, CA, 1997.
- (10) Kegley-Owen, C. S.; Gilles, M. K.; Burkholder, J. B.; Ravishankara, A. R. *J. Phys. Chem. A* **1999**, *103*, 5040.
- (11) Litorja, M.; Ruscic, B. *J. Electron Spectrosc. Relat. Phenom.* **1998**, *97*, 131.
- (12) *Thermodynamic Properties of Individual Substances*, 4th ed.; Gurvich, L. V.; Veyts, I. V.; Alcock, C. B., Eds.; Hemisphere: New York, 1989; Vol. 1.
- (13) Carlone, C.; Dalby, F. W. *Can. J. Phys.* **1969**, *47*, 1945.
- (14) Ruscic, B.; Feller, D.; Dixon, D. A.; Peterson, K. A.; Harding, L. B.; Asher, R. L.; Wagner, A. F. *J. Phys. Chem. A* **2001**, *105*, 1. The values reported in this citation have since been revised slightly by the authors. The most current values are $\Delta_f H_0^{\circ}(\text{OH}) = 8.86 \pm 0.07 \text{ kcal mol}^{-1}$ and $\Delta_f H_{298}^{\circ}(\text{OH}) = 8.92 \pm 0.07 \text{ kcal mol}^{-1}$.
- (15) Berkowitz, J.; Ellison, G. B.; Gutman, D. *J. Phys. Chem. A* **1994**, *98*, 2745.
- (16) Moylan, C. R.; Brauman, J. I. *Annu. Rev. Phys. Chem.* **1983**, *34*, 187.
- (17) Mordaunt, D. H.; Ashfold, M. N. R. *J. Chem. Phys.* **1994**, *101*, 2630.
- (18) Bierbaum, V. M.; Schmitt, R. J.; DePuy, C. H.; Mead, R. D.; Schulz, P. A.; Lineberger, W. C. *J. Am. Chem. Soc.* **1981**, *103*, 6262.
- (19) Oakes, J. M.; Harding, L. B.; Ellison, G. B. *J. Chem. Phys.* **1985**, *83*, 5400.
- (20) Clifford, E. P.; Wenthold, P. G.; Gareyev, R.; Lineberger, W. C.; DePuy, C. H.; Bierbaum, V. M.; Ellison, G. B. *J. Chem. Phys.* **1998**, *109*, 10293.
- (21) Leopold, D. G.; Murray, K. K.; Miller, A. E. S.; Lineberger, W. C. *J. Chem. Phys.* **1985**, *83*, 4849.
- (22) Ramond, T. M. Negative Ion Photoelectron Spectroscopy of Peroxides, Alkoxides, and Group VIII Transition Metal Oxides. Ph.D. Dissertation, University of Colorado, Boulder, CO, 2001.
- (23) Cooper, J.; Zare, R. *J. Chem. Phys.* **1968**, *48*, 942.
- (24) Van Doren, J. M.; Barlow, S. E.; DePuy, C. H.; Bierbaum, V. M. *Int. J. Mass. Spectrom. Ion Processes* **1987**, *81*, 85.
- (25) Schalley, C. A.; Schroeder, D.; Schwarz, H.; Moebus, K.; Boche, G. *Chem. Ber./Recl.* **1997**, *130*, 1085.
- (26) Blanksby, S. J.; Kato, S.; Bierbaum, V. M.; Ellison, G. B., to be submitted for publication, 2002.
- (27) Perin, D. D.; Armarego, W. L. F.; Perrin, D. R. *Purification of Laboratory Chemicals*, 2nd ed.; Pergamon Press: Oxford, U.K., 1980.
- (28) Scratchard, G.; Kavanagh, G. M.; Ticknor, L. B. *J. Am. Chem. Soc.* **1952**, *74*, 3715.
- (29) Hunziker, H. E.; Wendt, H. R. *J. Chem. Phys.* **1974**, *60*, 4622.
- (30) Bernath, P. F. *Spectra of Atoms and Molecules*, 1st ed.; Oxford University Press: New York, 1995.
- (31) Jacox, M. E.; Milligan, D. E. *J. Mol. Spectrosc.* **1972**, *42*, 495.
- (32) McKellar, A. R. W. *J. Chem. Phys.* **1979**, *71*, 81.
- (33) Smith, D. W.; Andrews, L. *J. Chem. Phys.* **1974**, *60*, 81.
- (34) Blanksby, S. J.; Ramond, T. M.; Davico, G. E.; Nimlos, M. R.; Kato, S.; Bierbaum, V. M.; Lineberger, W. C.; Ellison, G. B.; Okumura, M. *J. Am. Chem. Soc.* **2001**, *123*, 9585.
- (35) Celotta, R. J.; Bennett, R. A.; Hall, J. L.; Siegel, M. W.; Levine, J. *Phys. Rev. A* **1972**, *6*, 631.
- (36) Ervin, K. M.; Gronert, S.; Barlow, S. E.; Gilles, M. K.; Harrison, A. G.; Bierbaum, V. M.; DePuy, C. H.; Lineberger, W. C.; Ellison, G. B. *J. Am. Chem. Soc.* **1990**, *112*, 5750.
- (37) Su, T.; Chesnavich, W. J. *J. Chem. Phys.* **1982**, *76*, 5183.
- (38) Cotton, F. A.; Wilkinson, G.; Murillo, C. A.; Bochmann, M. *Advanced Inorganic Chemistry*, 6th ed.; Wiley & Sons: New York, 1999.
- (39) Schalley, C. A.; Wesendrup, R.; Schroeder, D.; Schwarz, H. *Organometallics* **1996**, *15*, 678.
- (40) Scatterfield, C. N.; Yeung, R. S. C. *Ind. Eng. Chem. Fundam.* **1963**, *2*, 257.
- (41) Schulz, P. A.; Mead, R. D.; Jones, P. L.; Lineberger, W. C. *J. Chem. Phys.* **1982**, *77*, 1153.
- (42) *Gas-Phase Ion-Molecule Reaction Rate Constants Through 1986*; Ikezoe, Y., Matsuoka, S., Takebe, M., Viggiano, A., Eds.; Ion Reaction Research Group of the Mass Spectroscopy Society of Japan: Maruzen, Tokyo, 1986.
- (43) The thermochemistry of hydrogen peroxide and the associated uncertainties presented in this work rely heavily on the reference acid used in these kinetic measurements. It is therefore important to be clear as to the origin of the gas-phase acidity that we select for acetylene. Ervin et al.³⁶ conducted careful gas-phase acidity measurements, analogous to those described here, to determine a gas-phase acidity for acetylene of $\Delta_{\text{acid}}G_{298}^{\circ}(\text{HC}\equiv\text{C}-\text{H}) = 369.8 \pm 0.6 \text{ kcal mol}^{-1}$ using the well-established gas-phase acidity of HF as a reference. Since then, however, near-UV photolysis of acetylene¹⁷ has been used to measure the bond energy in acetylene, $D_0(\text{HC}\equiv\text{C}-\text{H}) = 131.73 \pm 0.02 \text{ kcal mol}^{-1}$, precisely. This bond energy may be converted to a gas-phase acidity using (i) the integrated heat capacity³⁶ (cf. eq 21) to derive the bond enthalpy, $DH_{298}^{\circ}(\text{HC}\equiv\text{C}-\text{H}) = 133.18 \pm 0.02 \text{ kcal mol}^{-1}$; (ii) the electron affinity, $EA(\text{HC}\equiv\text{C}^-) = 68.5 \pm 0.2 \text{ kcal mol}^{-1}$, to derive the enthalpy of deprotonation, $\Delta_{\text{acid}}H_{298}^{\circ}(\text{HC}\equiv\text{C}-\text{H}) = 378.3 \pm 0.2 \text{ kcal mol}^{-1}$ (cf. eq 6); and (iii) the entropy of deprotonation, $\Delta_{\text{acid}}S_{298}^{\circ}(\text{HC}\equiv\text{C}-\text{H}) = 26.8 \pm 0.5 \text{ cal mol}^{-1} \text{ K}^{-1}$ (cf. eq 19), which gives $\Delta_{\text{acid}}G_{298}^{\circ}(\text{HC}\equiv\text{C}-\text{H}) = 370.3 \pm 0.3 \text{ kcal mol}^{-1}$. It is pleasing that the new value falls within the stated uncertainty of the old; however, we choose the more precisely determined new value to anchor the thermochemistry in this work.